

Flexible network model to study the impact of future changes in transmission systems on harmonic levels and impedance

Ana Maria BLANCO	Max DOMAGK	Jan MEYER	Marco LINDNER
TUD Dresden University of Technology	TUD Dresden University of Technology	TUD Dresden University of Technology	TransnetBW GmbH
Germany	Germany	Germany	Germany
ana.blanco@ tu-dresden.de	max.domagk@ tu-dresden.de	jan.meyer@ tu-dresden.de	m.lindner@ transnetbw.de

SUMMARY

The vastly growth of power electronic installations, like HVDC converter stations, wind parks, solar farms, FACTS, etc., has significantly increased the interest of harmonic studies in transmission systems. Harmonic studies in transmission systems have considerable challenges, mainly due to the complexity of the network (meshed network topology, realistic modelling of transmission lines and assets), the lack of information about parameters of network elements as well as the harmonic emission and impedance of connected customers or downstream networks, especially in case of unbalanced conditions.

In order to study different aspects related to harmonics, like the impact of the downstream networks on the harmonic levels in transmission systems, the impact of the transition to inverter-based resources, the influence of transmission line modelling detail or the validation of methods for assessing the harmonic emission of customers, a test network has been developed and continuously improved over the last five years. The test network consists of an extra high voltage network, which is formed by three interconnected regions with a nominal voltage of 380 kV and 220 kV. Two downstream 110 kV networks (one in a 380 kV region and one in a 220 kV region) are modelled in detail, to allow studies of the interaction between distribution and transmission systems, e.g. in terms of propagation or allocation of emission limits. The test network is developed in cooperation with the German Transmission System operators and is parametrized in order to represent the frequency-dependent impedance of all network components as realistic as possible. The test network represents typical characteristics of meshed transmission networks in central Europe.

The first part of the article introduces and describes the test network in detail. The second part presents two examples of how the test network has been used to study practical research questions. The first example discusses the impact of inverter-based resources on harmonic impedance and propagation. The results show that inverter-based resources has a high impact on zero sequence impedances and harmonic influence coefficients, which quantify the propagation between network nodes. This is because inverter-based resources have not only a different impedance curve compared to conventional synchronous generators, but can also considerably change grounding conditions of the network.

The second example discusses the impact of transmission line characteristics on harmonic impedance and propagation. The results show that the tower geometry and transposition configuration have a

considerable impact on harmonic impedance and harmonic influence coefficients. The impact is higher for zero sequence impedances. The study also shows that in case of asymmetrical geometry conditions, a coupling exists between the impedance sequences. This means that balanced current harmonic injections can result in unbalanced voltage harmonics in the network.

The paper concludes by discussing the potential of the test network to study other factors that affect harmonic propagation. Future work will focus on studying the impact of the characteristics of transformers, downstream distribution networks, customer installations, and power electronic based generation on harmonic impedances and propagation.

KEYWORDS

harmonic impedance, harmonic propagation, harmonic models, transmission system, inverter-based resources, transmission line modelling

1. TEST NETWORK

A model of a typical transmission network is developed in cooperation with the four German transmission systems operators (TSO) taking as reference the PST-16 benchmark network presented in [1]. The network elements are modeled in detail in order to represent their frequency dependent parameters based on the recommendation of [2]. The results of the fundamental power flow have been analyzed in order to verify the proper operation of the test network. This included the voltage band compliance and the loading of the network elements. Moreover, the resulting network harmonic impedances have been compared with some available measurements to ensure plausibility and qualitative consistency.

1.1 Network topology

The test network is shown in Figure 1. The network is divided into three regions and has two extra high voltage levels (380 kV and 220 kV). The network features 43 overhead lines, with 20 and 23 lines at 380 kV and 220 kV voltage levels respectively. Furthermore, the network includes 16 generators, 5 compensation devices and a total of 34 loads, which represent 110 kV downstream networks connected to the 380 kV and 220 kV levels through transformers. Two 110 kV networks are modelled in detail.

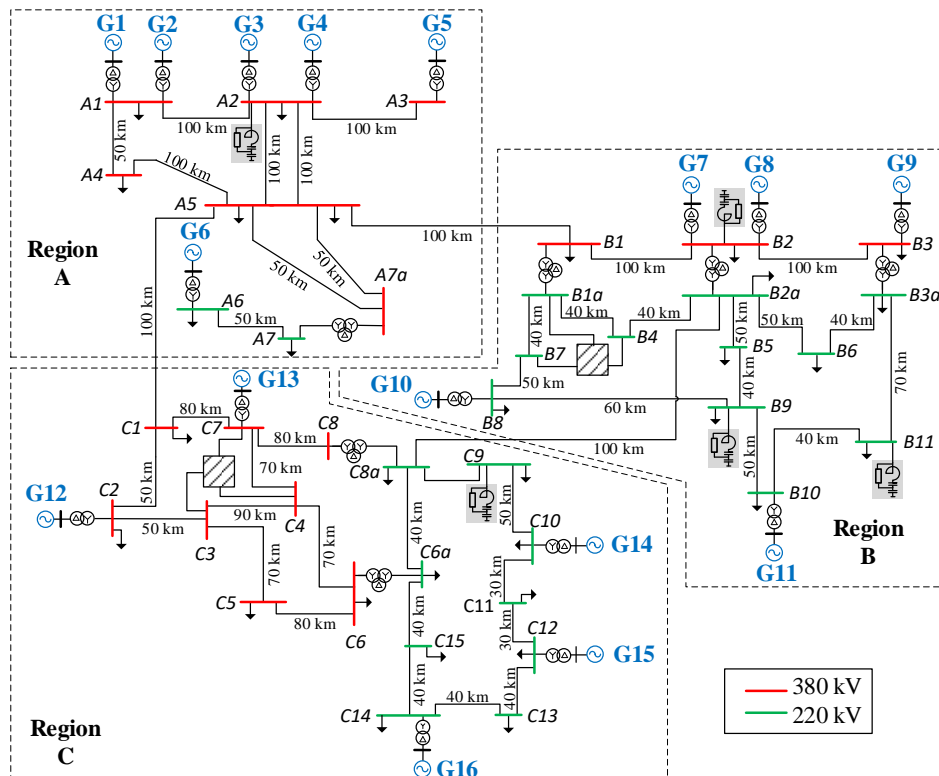


Figure 1: Test network for the harmonic analysis of transmission networks

1.2 Network elements

Overhead lines

All overhead lines are modelled in detailed using the geometry of the transmission towers and the characteristics of the conductors. All simulations are performed using the distributed parameters model (line equations) considering the skin effect in order to accurately capture the frequency-dependent characteristics of the transmission lines and the coupling between conductors. Based on this modeling approach, the positive, negative and zero sequence impedance can be determined.

Three different tower types, commonly used in German transmission networks are considered, as shown in Figure 2. In total three scenarios considering different tower geometries are defined:

- Mix: transmission lines are represented with tower type A with one or two circuits, i.e. this scenario considers a mix of lines with symmetrical and asymmetrical geometries.
- SGe (symmetrical geometries): All transmission lines are represented with tower type B with two circuits.
- AGe (asymmetrical geometries): All transmission lines are represented with tower type C.

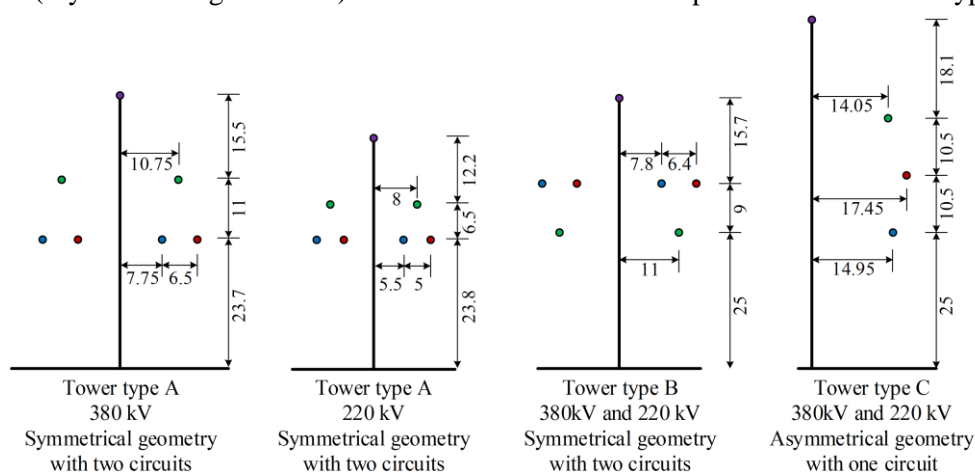


Figure 2: Tower geometries. All dimensions are given in meters. Tower type A is obtained from [3]

Additionally, two configurations with different transposition configurations are considered:

- Perf (perfect transposition): All phases of all circuits occupy all possible conductor position combinations. There will be no mutual coupling neither within a circuit nor between circuits. If only one side of the tower is used (i.e. one circuit), then the transposition is applied between the phases of the circuit.
- None (no transposition): The circuits are not transposed and each conductor of the circuit maintains its position for the entire length of the line. There will be mutual coupling within each circuit as well as between the circuits.

The two configurations used here represent the best-case and worst-case regarding transposition.

Transformers

The positive and negative sequence impedances (short-circuit voltage and copper losses) of the transformers have been reviewed and adjusted in accordance with the reference values provided in [3]. The zero sequence impedance is estimated based on some reference values obtained from real transformers. However, the transformer's switching group, the core type (3-leg or 5-leg core) and the star-point grounding characteristics affect the zero sequence equivalent impedance of the transformer.

All transformers are 5-leg transformers. All transformers between voltage levels (380 kV/220 kV, 380 kV/110 kV, and 220 kV/110kV) are configured in a star-star connection with an additional delta-winding (YNynd0). The transformers connecting the generators to the grid are connected in a star-delta configuration (Yd5). Some transformer neutral points are solidly grounded. The transformers with grounding connection has been selected in order to keep the earth fault factors at all 380 kV and 220 kV nodes in the range of 1.1 to 1.4 (operational optimum).

Compensation devices

Five compensation devices are located at different nodes in the 380 kV and 220 kV networks (c.f. nodes A2, B2, B9, B11 and C9 in Figure 1). The size of the compensation devices is selected in order to reduce the loading of the generators.

Generation

Synchronous generators

The synchronous generators are modelled using passive impedances for all sequence components [2]. The values of these impedances are calculated based on rated apparent power, rated voltage, power factor, stator resistance, sub-transient reactance, and data related to the negative sequence component. In total 16 generators are located at different nodes in all three regions (c.f. Figure 1 generators G1 to G16). Each generator is connected to the network through a transformer with a star-delta configuration (Yd5).

Inverter-based resources

Models of two different inverter-based resources (IBR) are also implemented in order to simulate different generation configurations in the test network. The frequency-dependent input impedance of the IBRs represents the impedance characteristics of two different modular multi-level converters (MMC). The MMC type 1 and MMC type 2 are modelled using measured impedances from [4] and [5], which include the impedance of the interface transformer. The positive sequence impedances of both types of MMCs are shown in Figure 3 (the negative sequence has the same values).

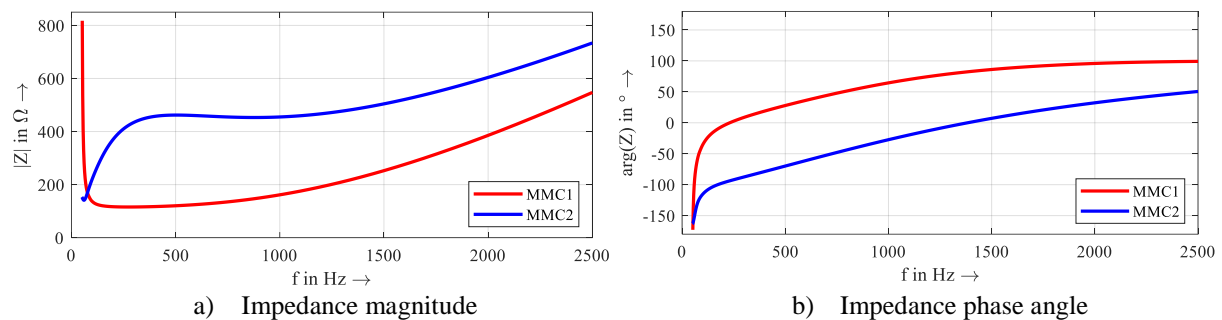


Figure 3: Frequency-dependent impedances for generic MMCs (MMC type 1 [4] and MMC type 2 [5])

No specific information about the zero sequence impedance characteristic of MMCs could be found in the literature. However, the zero sequence impedance of a MMC is mainly determined by the characteristics of the interface transformer, namely the leg type (3-leg or 5-leg transformer), the winding connection (Yy, Yd, Dy) and the grounding of the neutral point of star-connected windings. In the test network all MMCs have an interface transformer with 5 legs, Yd winding connection (delta winding connected to the inverter) and the neutral point of the Y winding solidly grounded. With this configuration, the zero sequence impedance for the combination of interface transformer and MMC seen from the grid-side is modelled being approximately equivalent to the positive sequence impedance of the interface transformer [6].

Loads

The loads represent downstream 110 kV networks, but they could also represent other type of users connected directly to the transmission network. Initially, two different impedance models, IEEE load model 1 (RL in series) and IEEE load model 2 (RL in parallel), are employed [7]. These are connected on the 110 kV side of the 380 kV/110 kV or 220 kV/110 kV transformers. The loads usually also include capacitances. Suitable options to include these capacitances are currently under research.

Two 110 kV networks are modelled in detail in order to analyze the impact of downstream distribution network modeling on harmonic propagation within the transmission system. The network topology is based on [8] and has been adjusted to reflect the typical loading conditions of 110 kV networks in Germany. The first 110 kV network is interconnected with the 220 kV network (nodes B1a, B4, B7), while the second 110 kV network is connected to the 380 kV network (nodes C3, C4, C7). Both 110 kV

networks share the same configuration, as depicted in Figure 4. The loads of the detailed 110 kV networks are connected via transformers and they represent the aggregated 20 kV networks. These loads are modeled using the CIGRE load model presented in [9].

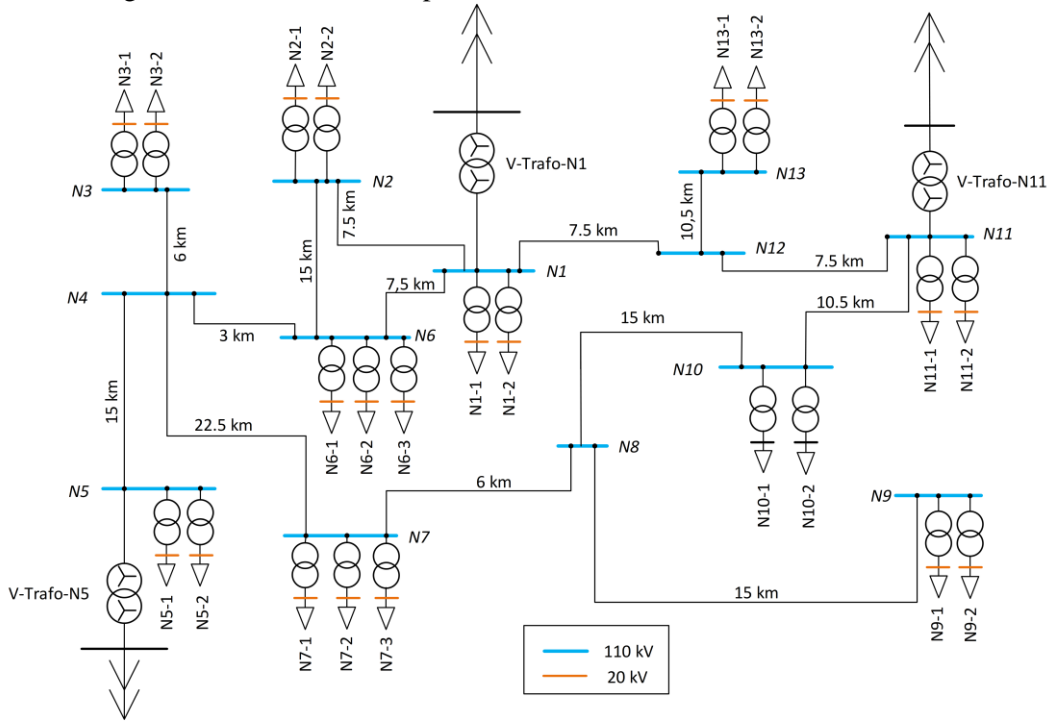


Figure 4: Detailed model of 110 kV network

1.3 Reference scenario

The reference scenario of the test network considers a transmission system with exclusively synchronous generators and symmetric tower geometries (Scenario SGe) with perfect transposition of the conductors. Moreover, all loads are modeled using the IEEE load model 2.

2. HARMONIC NETWORK CHARACTERISTICS

Harmonic network characteristics distinguish between the harmonic (node) impedance at a single node and the harmonic propagation characteristics between any two nodes, which is expressed by harmonic influence coefficients. To determine the harmonic network characteristics, a harmonic current of order $h = 2, \dots, 50$ with a constant amplitude $I_{s,i}^{(h)} = 1$ A and the sequence s (positive (+), negative (-) or zero (0)) is injected individually into node i . Depending on the effective harmonic impedances of the network, this results in a harmonic voltage $\underline{U}_{s,j}^{(h)}$ at node j for each sequence component s . For N nodes, the voltage vector for each harmonic order (h) and sequence (s) is given by:

$$\underline{\mathbf{U}}_s^{(h)} = \left[\underline{U}_{s,1}^{(h)}, \underline{U}_{s,2}^{(h)}, \dots, \underline{U}_{s,j}^{(h)}, \dots, \underline{U}_{s,N}^{(h)} \right]^T \quad \text{with } s = +, -, 0 \quad (1)$$

It should be noted that despite at the sending node only one sequence is injected at a time, at the receiving node voltages in all sequences can occur due to unbalances in the network.

2.1 Network harmonic impedance

Based on the injected harmonic current $I_{+,i}^{(h)}$ at node i and the measured harmonic voltage $\underline{U}_{+,i}^{(h)}$ the network harmonic impedance of the positive sequence is determined by:

$$\underline{Z}_{++,i}^{(h)} = \frac{\underline{U}_{+,i}^{(h)}}{I_{+,i}^{(h)}} \quad \text{with } i = 1, \dots, N \quad (2)$$

Depending on the combination of the injected sequence system (current) and the measured sequence systems (voltage) this results in the impedance matrix:

$$\underline{Z}_i^{(h)} = \begin{bmatrix} \underline{Z}_{++ ,i}^{(h)} & \underline{Z}_{+- ,i}^{(h)} & \underline{Z}_{+0 ,i}^{(h)} \\ \underline{Z}_{-+ ,i}^{(h)} & \underline{Z}_{-- ,i}^{(h)} & \underline{Z}_{-0 ,i}^{(h)} \\ \underline{Z}_{0+ ,i}^{(h)} & \underline{Z}_{0- ,i}^{(h)} & \underline{Z}_{00 ,i}^{(h)} \end{bmatrix} \text{ with } i = 1, \dots, N \quad (3)$$

In case of a symmetric system and balanced conditions only the diagonal elements remain and the couplings between the sequences (off-diagonal elements) become zero (decoupled system).

2.2 Harmonic influence coefficients

The harmonic influence coefficients are efficient indices to study the propagation of harmonics within a network. These are defined in a similar manner as specified in IEC 61000-3-6 for determining harmonic distortion limits in interconnected high and extra-high voltage networks [10]. The harmonic current injected as a positive sequence at node i results in the harmonic voltage $\underline{U}_{+,i}^{(h)}$ at node i and the harmonic voltage $\underline{U}_{+,j}^{(h)}$ at any other node j within the network. The ratio of these two voltages forms the complex harmonic influence coefficient:

$$\underline{c}_{+,ij}^{(h)} = \frac{\underline{U}_{+,j}^{(h)}}{\underline{U}_{+,i}^{(h)}} \text{ with } i = 1, \dots, N \text{ and } j = 1, \dots, N \quad (4)$$

The magnitude of the coefficient indicates whether and to what extent the harmonic voltage caused by node i at node j is attenuated ($c < 1$) or amplified ($c > 1$) in relation to the voltage at node i . The phase angle of the harmonic influence coefficient corresponds to the phase shift between the harmonic voltages of node j and node i with respect to node i . In general, for all sequence systems a 3x3 matrix of harmonic influence coefficients can be determined for each harmonic order h and any combination of two nodes i and j :

$$\underline{c}_{ij}^{(h)} = \begin{bmatrix} \underline{c}_{++ ,ij}^{(h)} & \underline{c}_{+- ,ij}^{(h)} & \underline{c}_{+0 ,ij}^{(h)} \\ \underline{c}_{-+ ,ij}^{(h)} & \underline{c}_{-- ,ij}^{(h)} & \underline{c}_{-0 ,ij}^{(h)} \\ \underline{c}_{0+ ,ij}^{(h)} & \underline{c}_{0- ,ij}^{(h)} & \underline{c}_{00 ,ij}^{(h)} \end{bmatrix} \text{ with } i = 1, \dots, N \text{ and } j = 1, \dots, N \quad (5)$$

In case of a symmetric system and balanced conditions only the diagonal elements remain and the couplings between the sequences (off-diagonal elements) become zero (decoupled system).

3. EXAMPLE 1: REPLACEMENT OF CONVENTIONAL GENERATION BY INVERTER-BASED RESOURCES

The integration of renewable energy into the transmission system (e.g. large wind and solar farms) results in a continuous change from conventional generation based on synchronous generators (SG) towards inverter-based resources (IBR). This development is expected to change both harmonic impedances and harmonic levels in the transmission system.

3.1 Scenarios

In order to analyze the transition from conventional generation to IBR, 60 % of the SGs of the reference scenario are replaced by IBRs according to Table 1. Refer to section 1.2 for further details on the different generator models.

Table 1: Generation scenario. SG: Synchronous generator, M1: MMC type 1, M2: MMC type 2.

Generator	G1	G2	G3	G4	G5	G6	G7	G8	G9	G10	G11	G12	G13	G14	G15	G16
Node	A1	A1	A2	A2	A3	A6	B2	B2	B3	B8	B10	C2	C7	C10	C12	C14
Ref. scenario	SG	SG	SG	SG	SG	SG	SG	SG	SG	SG	SG	SG	SG	SG	SG	SG
IBR scenario	M1	SG	SG	SG	M2	M2	SG	M2	M1	M1	SG	M1	M2	M1	SG	M2

The active and reactive power generation values for each IBR are obtained from the load flow simulation of the reference scenario. Due to the replacement of SG by IBR, the short-circuit currents are affected. Consequently, the grounding configuration has been reconfigured in the IBR scenario in order to fulfill

the requirements for the earth fault factors as discussed in section 1.2 (transformers). This means that for the IBR scenario not only the type of generators changes, but also the grounding configuration. For the sake of simplicity only balanced conditions are considered in this example, which means only the diagonal elements of the matrices in (3) and (5) are analyzed.

3.2 Network harmonic impedance

Figure 5 shows exemplarily the network harmonic impedance (elements $Z_{+++,i}^{(h)}$ and $Z_{00,i}^{(h)}$ of eq. (3)) at three nodes and both scenarios. The nodes are selected as they represent the impedance variation of most of the nodes in the three regions. The negative sequence impedances are not shown as they have similar values as the positive sequence impedances. In most of the cases there is a significant decrease or increase of the magnitude of the impedance, especially at the resonance frequencies. For example for the zero sequence impedance of node C5 around the 3rd harmonic order a clear shift of the resonance frequency is recognizable. A clear increase or decrease of the impedance with the change of the type of generators cannot be concluded. Moreover, high variations of the impedances can be found not only at nodes with replaced generators (e.g. node A3), but also at nodes without generation (e.g. node C5).

In order to evaluate the variation of the network harmonic impedance at all nodes, the difference of the impedance magnitudes obtained in both scenarios is calculated as following:

$$\Delta Z_{s,i}^{(h)} = \left| Z_{s,i,IBR}^{(h)} \right| - \left| Z_{s,i,REF}^{(h)} \right| \quad (6)$$

with the $Z_{s,i,IBR}^{(h)}$ representing the impedance for the IBR scenario at node i of sequence s ($++,-,00$) and harmonic order h and $Z_{s,i,REF}^{(h)}$ being the respective impedance of the reference scenario. The results obtained for all nodes and all harmonic orders are presented in heat maps, as shown in Figure 6. A negative value (blue colors) indicates that the impedance obtained in the IBR scenario is lower than the one obtained in the reference scenario. An increase of the impedance is indicated with red colors. All the impedances are referred to the 380 kV side.

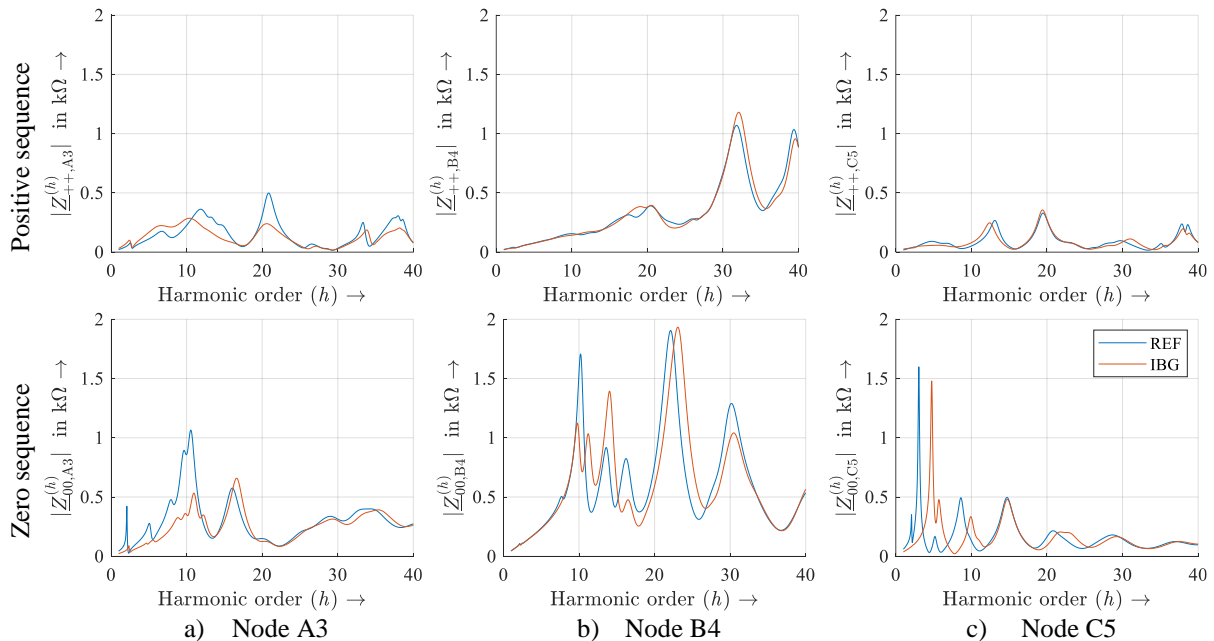


Figure 5: Positive and zero sequence harmonic impedances at nodes A3, B4 and C12 obtained in scenarios Reference scenario and IBR scenario

The heat maps show that the zero sequence impedance has a higher variation, especially at the 220 kV nodes. The variations of the positive sequence impedances are below 200 Ω , while the variations of the zero sequence impedances get values above 800 Ω . Variations of the impedance can be found in nodes with generation or no generation. However, additional simulations corroborate that the variation of the

zero sequence impedance is mainly determined by the change of the grounding configuration, and not by the change of the type of generation.

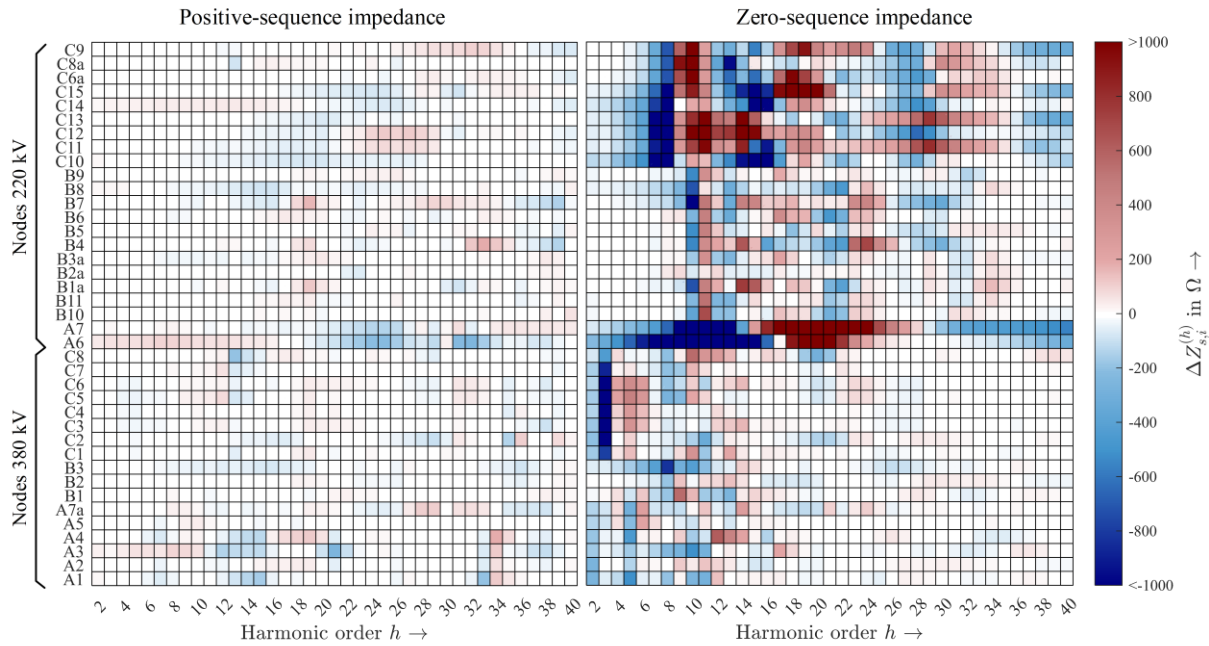


Figure 6: Difference of the harmonic impedance magnitude between the reference scenario and the IBR scenario for all nodes.

3.3 Harmonic influence coefficients

Figure 7 compares exemplarily the harmonic influence coefficients of the positive sequence for the 21st harmonic ($c_{++ij}^{(21)}$) obtained with the reference and the IBR scenarios. The plot indicates with colors the range in which each of the harmonic influence coefficients between two nodes varies. If a voltage harmonic is attenuated, the color in the graph is in the yellow-green range. If the voltage harmonic is amplified, the color is in the blue-red range. The elements of the diagonal are always one, and are therefore displayed in white. The two graphs are in general very similar for most nodes, but variations at some nodes are clearly recognizable (e.g nodal pairs C1-C2, C3-C7). There is not always an attenuation of the harmonics, but depending on the impedance characteristics amplifications can be also obtained between nodes.

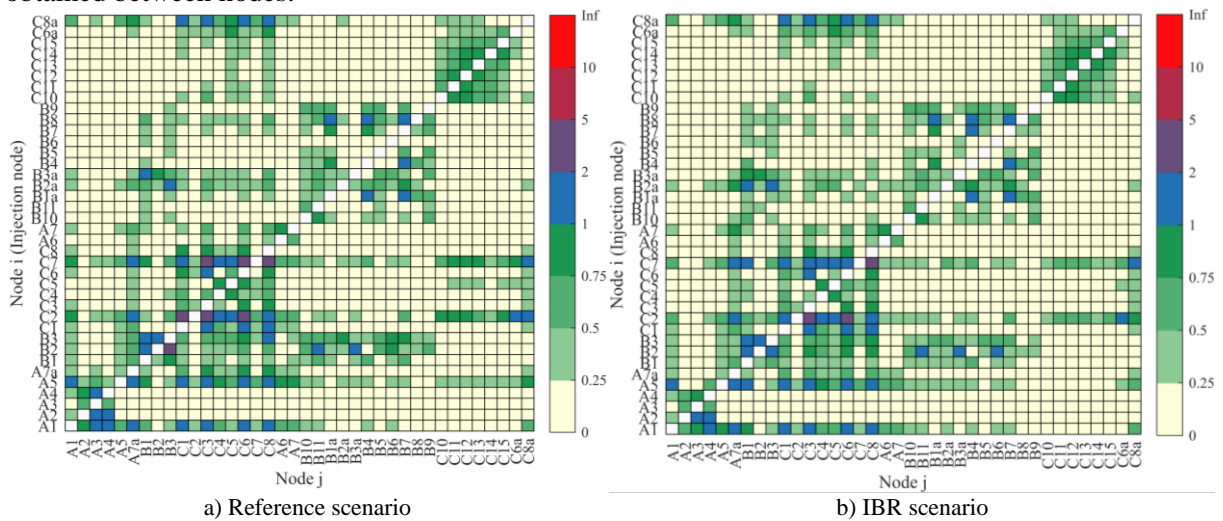


Figure 7: Harmonic influence coefficients $c_{++ij}^{(21)}$ obtained in the Reference scenario and IBR scenario

In order to facilitate the analysis for other harmonic orders, the difference between the harmonic influence coefficients obtained in both scenarios is calculated as follows:

$$\Delta c_{s,ij}^{(h)} = |\underline{c}_{s,ij,IBR}^{(h)}| - |\underline{c}_{s,ij,REF}^{(h)}| \quad (7)$$

Figure 8 summarizes the difference of the magnitudes of the harmonic influence coefficients obtained for all nodes between the reference and the IBR scenarios. The results are represented as a box plot where each box represents the distribution of the $\Delta c_{s,ij}^{(h)}$ between all nodes and for each harmonic order. In each box, the extreme top and bottoms are the 1st and 99th percentile values respectively, and inner filled box is bound by 95th and 5th percentile values. The black dash in the box represents the median.

The highest differences are obtained for zero sequence harmonics, which is related to the higher variation of the zero sequence harmonic impedance. However, the difference between the maximum value and the 95th percentile is very high, which indicates that the highest $\Delta c_{kj}^{(h)}$ values correspond to just a few nodes. Considering the 5th and 95th percentiles (filled boxes), the variation of the harmonic influence coefficients between the reference and the IBR scenarios is mostly below 0.6 p.u.. For most harmonics most of the differences $\Delta c_{kj}^{(h)}$ are below 0, which indicates that the harmonic influence coefficients tend to be lower for the scenario IBR, which means slightly more damping with regard to the propagation of harmonics in the network.

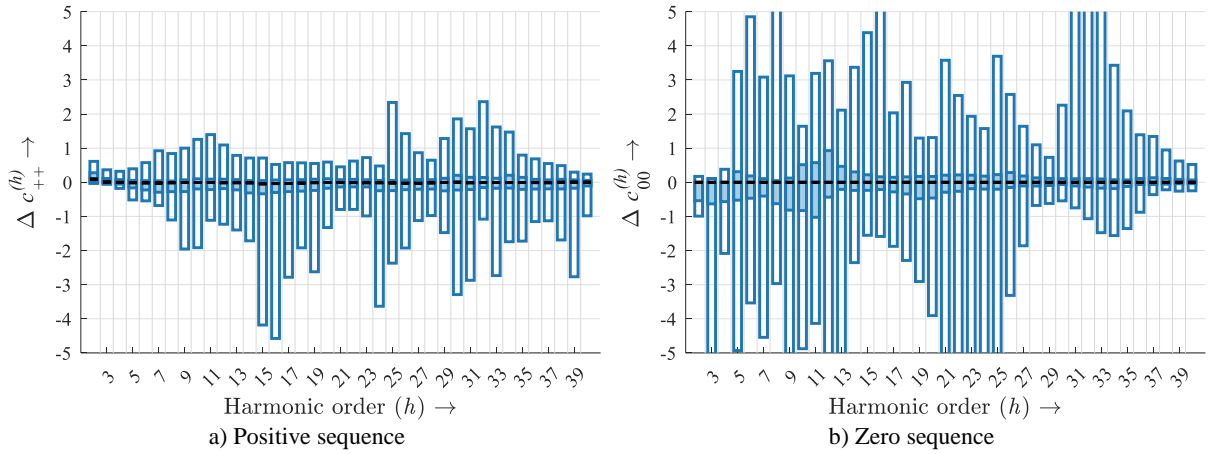


Figure 8: Absolute difference of the harmonic influence coefficients between the reference and the IBR scenario.

4. EXAMPLE 2: IMPACT OF TRANSMISSION LINE CHARACTERISTICS

The characteristics and configuration of the network elements like lines or transformers can influence harmonic impedance and propagation behavior in a network. Some characteristics have a greater impact than others. As example, the sensitivity the impact of geometry and transposition of transmission lines is studied.

4.1 Scenarios

In total six scenarios are defined using all combinations for the configurations of tower geometry and transposition of conductors as described in section 1.2. These scenarios are listed in Table 2.

Table 2: Scenarios for the analysis

Scenario	Tower geometry	Transposition
SGe-Perf (Ref)	Symmetrical	Perfect
SGe-None		None
Mix-Perf	Symmetrical und Asymmetrical	Perfect
Mix-None		None
AGe-Perf	Asymmetrical	Perfect
AGe-None		None

4.2 Network harmonic impedance

The impedance is strongly affected by the tower geometry. Figure 9 shows exemplarily the magnitude of the harmonic impedances at node C5 (central node in Region C) for all scenarios. The figures on the left show the diagonal elements $Z_{++}^{(h)}$ and $Z_{00}^{(h)}$ (self-impedances) as defined in eq. (3), while the figures on the right show the non-diagonal elements $Z_{+-}^{(h)}$ and $Z_{0+}^{(h)}$ (coupling-impedances). The coupling-impedances between sequence components have a value just for the scenarios with no transposition, i.e. in the scenarios with unbalanced conditions between the conductors. These mutual impedances have a lower value than the self-impedances (ratio 10:1), but in unbalanced conditions they play an important role regarding the propagation of harmonics.

Regarding the self-impedances, the highest differences are found at the resonance frequencies, where the geometry affects not only the magnitude but also the frequency of the resonance. Scenario SGe-Perf shows in this case the lowest magnitude of the harmonic impedance, especially at the zero sequence.

The transposition of the conductors has a lower impact than the geometry of the transmission tower.

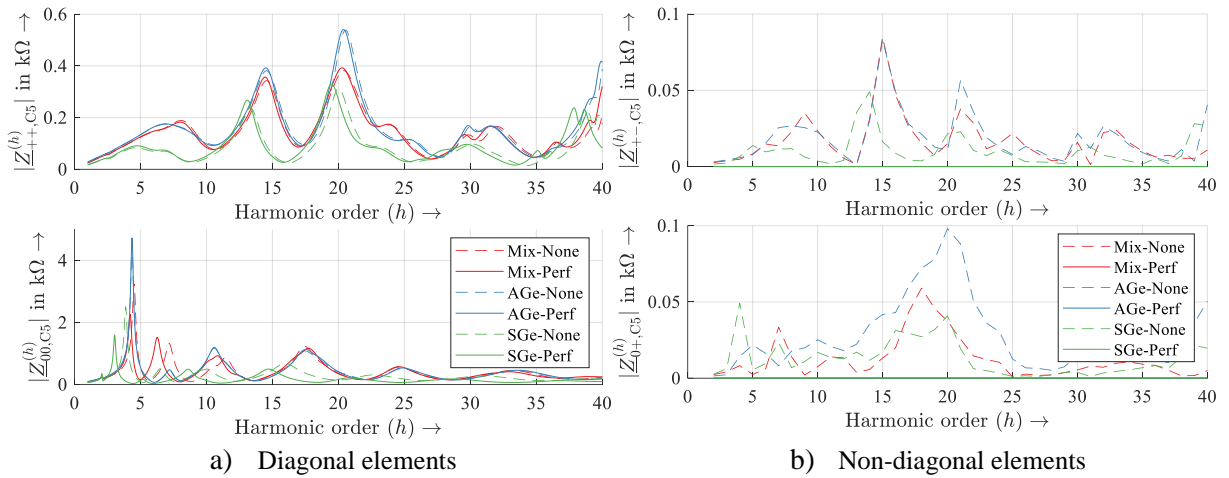


Figure 9: Magnitude of the positive and zero sequence harmonic impedance at node C5

In order to compare the variations of the impedance magnitudes for all the other nodes, the difference of the impedance magnitudes is calculated in the same way as in section 3. Only the diagonal elements (self-impedances) are considered for this analysis. The difference between different scenarios is calculated in order to analyze the effect of the geometry of the tower and the transposition separately. The results of the comparisons are summarized in Figure 10 using similar boxplots as in Figure 8, which aggregate the differences obtained for all nodes and all harmonic orders.

It is clear that the tower geometry (red boxplots) has a greater impact on the harmonic impedance than the transposition configuration (blue boxplots). However, the impact of the transposition configuration is not negligible, especially for the zero sequence impedance.

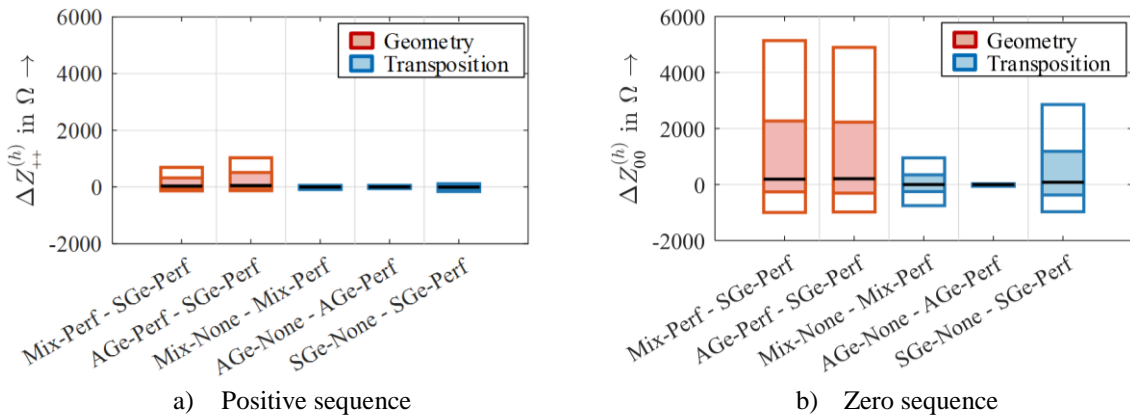


Figure 10: Differences of the impedance magnitude for all scenarios including all harmonic orders and all nodes for the positive sequence (a) and negative sequence (b).

4.3 Harmonic influence coefficients

The difference of the harmonic influence coefficients between the six scenarios are calculated in a similar way as described in section 3 and presented as boxplots similar to Figure 8. Figure 11 shows exemplarily the variation of the harmonic influence coefficients of the positive sequence and zero sequence between the scenarios SGe-Perf (reference) and AGe-Perf. Once again the positive sequence shows lower variations than the zero sequence, which is linked to the higher variation of the zero sequence harmonic impedance.

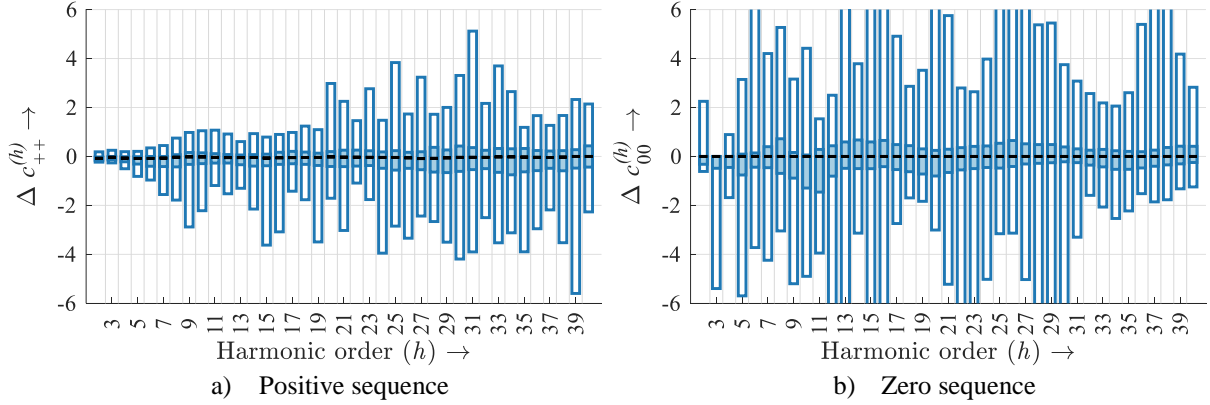


Figure 11: Absolute difference of the harmonic influence coefficients between scenarios SGe-Perf (Ref.) and AGe-Perf

A clear increase or decrease of the harmonic influence coefficients with the change of the geometry cannot be concluded. Like for the network harmonic impedance, the transposition of the lines has a lower impact on the harmonic influence coefficients than the geometry of the transmission tower.

5. CONCLUSIONS

A test network for harmonic analysis of transmission systems is developed with the cooperation of the German Transmission System operators. The model and parameters of the network elements are carefully chosen, in order to represent the frequency-dependent impedances of the network elements (transformers, transmission lines and generators) as realistic as possible. The test network can be used to make different studies related to harmonic emission and propagation in transmission systems to derive guidance on the design of future transmission systems and components considering an effective management harmonic levels.

Two exemplary applications of the test network are presented. The first example discusses the impact of the replacement of conventional generation based on synchronous generators by inverter-based resources on the network harmonic impedance and the propagation of harmonics. The results show a higher impact on the zero sequence impedances and harmonic influence coefficients, which is caused not only by the change of the impedance of the generators, but also due to the consequently required changes in the grounding configuration. The second example discusses the impact of geometry and transposition of the transmission lines on the harmonic impedance and the harmonic propagation. Both, tower geometry and transposition configuration have a considerable impact on the network harmonic impedance as well as the harmonic influence coefficients and consequently also the harmonic power flow. The impact of tower geometry is higher than that of the transposition configuration. The impact is not the same for all harmonic orders, and zero sequence harmonics showed the highest sensitivity. The example has further shown that the asymmetry of the transmission lines (no transposition of the conductors) results in a coupling between the impedance sequences and consequently balanced current harmonic injections can result in unbalanced voltage harmonics in the network.

The results of the two examples show the complexity of the interaction of harmonics transmission networks. Changes in the network topology or/and the network elements might result in completely different harmonic impedances and harmonic propagation behavior. Even small changes at one node or one network element can affect the behavior at multiple other nodes not necessarily located in close proximity. Therefore, assumptions and simplifications (e.g. limitation of considered nodes) should be

carefully assessed for harmonic studies in transmission systems. Finally the inherent unbalance of the transmission system in terms of network elements as well as harmonic sources cannot be neglected for realistic studies.

Moreover, the impact of the characteristics of other network elements, as the transformers, the downstream distribution networks, the customer installations and the power electronic based generation on harmonic impedance, propagation and power flow can be also studied using the test network. Future work is dedicated to the continuous improvement and validation of the test network, especially focusing on the modelling of downstream networks and customer installations.

BIBLIOGRAPHY

- [1] S. P. Teeuwesen, I. Erlich, M. A. El-Sharkawi and U. Bachmann, "Genetic algorithm and decision tree based oscillatory stability assessment," *2005 IEEE Russia Power Tech*, St. Petersburg, Russia, 2005, pp. 1-7, doi: 10.1109/PTC.2005.4524480.
- [2] CIGRE Joint Working group C4/B4.38, "Network modelling for harmonic studies. Technical Brochure 766", CIGRE, 2019.
- [3] D. Oeding and B. R. Oswald, *Elektrische Kraftwerke und Netze*, Berlin Heidelberg: Springer-Verlag, 2011.
- [4] D. Yang, X. Wang, M. Ndreko, W. Winter, R. Juhlin and A. Krontiris, „Automation of Impedance Measurement for Harmonic Stability Assessment of MMC-HVDC Systems,“ in *9th Solar & 18th Wind Integration Workshops 2019*, Dublin, Ireland, 2019.
- [5] S. Wenig, C. Hirsching, C. John and T. Leibfried, „Considerations on the frequency-dependent grid impedance in meshed HVAC grids - Parametric sensitivity analysis and impact of power electronic assets,“ in *In Proceedings of the 48th CIGRE Paris Session*, Paris, France, 2020.
- [6] L. Hoffmann. *Elektrische Energieversorgung – Band 2: Betriebsmittel und ihre quasistationäre Modellierung (Electrical power supply - Volume 2: Equipment and its quasi-stationary modeling)*, Berlin/Boston: Walter de Gruyter GmbH, 2019
- [6] R. Burch et al., 'Impact of aggregate linear load modeling on harmonic analysis: a comparison of common practice and analytical models', *IEEE Trans. Power Delivery*, vol. 18, no. 2, pp. 625–630, Apr. 2003, doi: 10.1109/TPWRD.2003.810492.
- [7] D. Chakravorty, J. Meyer, and P. Schegner, 'Aspects of network harmonic impedance modelling in high voltage distribution networks', in *2013 IEEE Power & Energy Society General Meeting*, IEEE, 2013, pp. 1–5. doi: 10.1109/PESMG.2013.6672866.
- [8] CIGRE WG 36-05, "Harmonics, characteristic parameters, methods of study, estimates of existing values" *Electra* 77, July 1981.
- [9] IEC TR 61000-3-6, 'Electromagnetic compatibility (EMC) - Part 3-6: Limits - Assessment of emission limits for the connection of distorting installations to MV, HV and EHV power systems', IEEE, 2008.